Hydrology and
Earth System
Sciences

In situ unsaturated zone water stable isotope (^{2}H and ^{18}O) measurements in semi-arid environments: a soil water balance

Marcel Gaj[1,2], **Matthias Beyer**[1], **Paul Koeniger**[1], **Heike Wanke**[3], **Josefina Hamutoko**[3], and **Thomas Himmelsbach**[1]

[1]Federal Institue for Geosciences and Natural Resources (BGR), Stilleweg 2, Hanover, Germany
[2]Chair of Hydrology, Faculty of Environment and Natural Resources, University of Freiburg,
Fahnenbergplatz, 79098 Freiburg, Germany
[3]Department of Geology, University of Namibia (UNAM), Windhoek, Namibia

Correspondence to: Marcel Gaj (marcel.gaj@bgr.de)

Abstract. Stable isotopes (deuterium, ^{2}H, and oxygen-18, ^{18}O) of soil water were measured in the field using a liquid water isotope analyzer (tunable off-axis integrated cavity output spectroscope, OA-ICOS, LGR) and commercially available soil gas probes (BGL-30, UMS, Munich) in the semi-arid Cuvelai–Etosha Basin (CEB), Namibia. Results support the applicability of an in situ measurement system for the determination of stable isotopes in soil pore water. High spatial and temporal resolution was achieved in the study area with reasonable accuracy and measurements were in agreement with laboratory-based cryogenic vacuum extraction and subsequent cavity ring-down laser spectroscopic isotope analysis (CRDS, L2120-i, Picarro Inc.). After drift and span correction of the in situ isotope data, precision for over 140 measurements taken during two consecutive field campaigns (June and November 2014) was 1.8 and 0.48 ‰ for δ^2H and δ^{18}O, respectively. Mean measurement trueness is determined using quality check standards and was 5 and 0.3 ‰ for δ^2H and δ^{18}O, respectively. The isotope depth profiles are used quantitatively to calculate a soil water balance. The contribution of transpiration to total evapotranspiration ranged between 72 and 92 %. Shortly after a rain event, the contribution of transpiration was much lower, at 35 to 50 %. Potential limitations of such an in situ system are related to environmental conditions which could be minimized by using a temperature-controlled chamber for the laser spectrometer. Further, the applicability of the system using previously oven-dried soil material might be limited by physicochemical soil properties (i.e., clay minerals). Uncertainty in the in situ system is suggested to be reduced by improving the calibra-

tion procedure and further studying fractionation effects influencing the isotope ratios in the soil water, especially at low water contents. Furthermore, the influence of soil-respired CO_2 on isotope values within the root zone could not be deduced from the data.

1 Introduction

Water stable isotopes have been successfully used for decades as powerful proxies for the description of water fluxes such as infiltration in humid (Saxena, 1987) or semi-arid regions (e.g., Dincer et al., 1974; Allison and Hughes, 1983), evapotranspiration (e.g., Barnes and Allison, 1988, Wang et al., 2012; Dubbert et al., 2013; Skrzypek et al., 2015), plant root water uptake (e.g., Dawson and Ehleringer, 1991; Ehleringer and Dawson, 1992; Dawson, 1996; Yang et al., 2010), hydraulic redistribution (Dawson, 1993; Caldwell et al., 1998), and catchment hydrology (e.g., Sklash and Farvolden, 1979; Richard and Shoemaker, 1986; Tetzlaff et al., 2007; Kendall and McDonnell, 2012). Soil water stable isotopes provide information on flow pathways and mixing within the unsaturated zone (e.g., Gazis and Feng, 2004; Stumpp and Maloszewski, 2010; Garvelmann et al., 2012; Mueller et al., 2014). Soil water stable isotope studies have also been used to reduce parameter uncertainty in unsaturated zone model approaches (Sprenger et al., 2015). Further work has been done to use soil water stable isotopes for quantitative recharge estimations (e.g., Beyer et al., 2015), which are actively discussed in earlier and recent reviews (e.g., Al-

lison et al., 1994; Scanlon et al., 2002; Koeniger et al., 2016). However, the usefulness of evaporation profiles to determine recharge rates remains debatable (Herczeg and Leany, 2011).

In most unsaturated zone studies, manual removal of soil samples and a subsequent extraction of soil water in the laboratory was necessary using vacuum extraction (e.g., West et al., 2006; Koeniger et al., 2011; Orlowski et al., 2013), equilibration (e.g., Wassenaar et al., 2008), mechanical squeezing, azeotropic distillation, or centrifugation methods (e.g., Walker et al., 1994; Kelln et al., 2001). These methods cause both disturbance to the integrity of the natural soil system and possible evaporation during the sampling procedure. The latter is especially important for dry soils. Hence, soil water extraction techniques are labor intensive and expensive, which limits the use of stable isotopes compared to the other variables, such as soil moisture or matrix potential measurements. Indeed, there are suction cup installations which allow a removal of soil water non-destructively, but they are not applicable in (semi-)arid environments. This is especially true during the dry season, when vapor transport (i.e., evaporation) is the dominant driver for water fluxes in the unsaturated zone, but the vapor transport is much less studied than the liquid water component (Soderberg et al., 2012). In this context, the determination of stable isotopes from sampling the vapor of the pore space appears useful.

Principles for sampling soil air for the determination of stable isotopes have already been indicated by Allison et al. (1987) and Schack-Kirchner et al. (1993). An attempt to measure stable isotopes in a sandy loam using a liquid water analyzer (OA-ICOS, Los Gatos Research, DLT-100) is presented in a recent review by Soderberg et al. (2012). The first study monitoring stable isotopes in situ in unsaturated sandy soil water under laboratory conditions made use of polypropylene (PP) membranes (Rothfuss et al., 2013). Measurements were performed with a cavity ring-down spectrometer (CRDS) (L1102-I, Picarro, CA, USA) calibrated with liquid water injections using a vaporizer unit. More recently they presented a long-term application of their in situ system under laboratory conditions (Rothfuss et al., 2015). Volkmann and Weiler (2014) developed their own polyethylene (PE) probes with an equilibration chamber allowing additional mixing of the vapor to prevent condensation in the sample line. They further proposed a sophisticated system with a CRDS device (Picarro L2120-i, CA, USA) calibrated with standards added to previously oven-dried substrate from their study site.

In the present study in situ usability of commercially available PP membranes (BGL-30, Umweltmesssysteme, Munich) using a liquid water analyzer (Los Gatos Research, DLT-100) for a determination of stable isotopes in soil pore water is demonstrated. The proposed system is applied under harsh remote field conditions in a semi-arid environment in soil with moisture contents ranging from 0.3 to 6 %. In comparison to earlier in situ studies this study presents the following:

i. We detail an improved automatization with minimal technical modification of commercially available parts.

ii. We demonstrate that in situ measurements are comparable to data derived from cryogenic vacuum extractions, as well as that there are differences at the transition to the atmosphere, which will be discussed. Such a comparison seems to be useful since the cryogenic soil water extraction allows a direct determination of the soil water isotopic composition.

iii. Finally, derived isotope data are used quantitatively to determine the soil water balance of a deep sandy unsaturated zone and for the partitioning of transpiration and evaporation.

2 Study site and methods

The study area is located in northern central Namibia and is part of the Cuvelai–Etosha Basin (CEB). The whole surface water catchment has an extent of about $173\,000\,\mathrm{km}^2$ where the northern part (approx. $52\,000\,\mathrm{km}^2$) belongs to Angola and the southern part to Namibia. This sedimentary basin is divided into four major sub-basins called Iishana, Niipele, Olushandja, and Tsumeb and can be further separated into different drainage zones. Measurements were conducted within the eastern sand zone close to the township of Elundu as indicated in Fig. 1. The assignment of the catchment and its sub-basins is based on geography, population distribution, and water infrastructure (Dragnich et al., 2004). The main shallow aquifer system in the CEB is a multilayer aquifer system in the Andoni formation with a thickness of 6 to 80 m. The main groundwater flow is towards the Etosha pan with an average gradient of 0.2 % (Christelis et al., 2001). In addition to the shallow aquifer, recent studies identified an area of $500\,\mathrm{km}^2$ potentially containing fresh groundwater at a depth of 200 m, named the Ohangwena II aquifer (Lindenmaier and Christelis, 2012; Lindenmaier et al., 2014). Groundwater recharge mechanisms concerning both the shallow and the deep aquifer are not yet fully understood. The shallow aquifer system consists partly of freshwater lenses on brackish to saline groundwater mostly in the Iishana region. Perched discontinuous aquifers are found in the eastern part of the basin that develop on clay lenses in the subsurface and are managed through hand-dug wells.

The climate in the CEB is semi-arid with a rainy season lasting from November to April and a dry season from May to October. Annual average potential evaporation can reach up to 3000 mm and decreases slightly from north to south (Mendelsohn et al., 2013). Annual average rainfall ranges between 250 and 600 mm, with most of the rain falling in January and February (Mendelsohn et al., 2013). The eastern part of the catchment receives more consistent rainfall, whereas rain in the western part is less predictable.
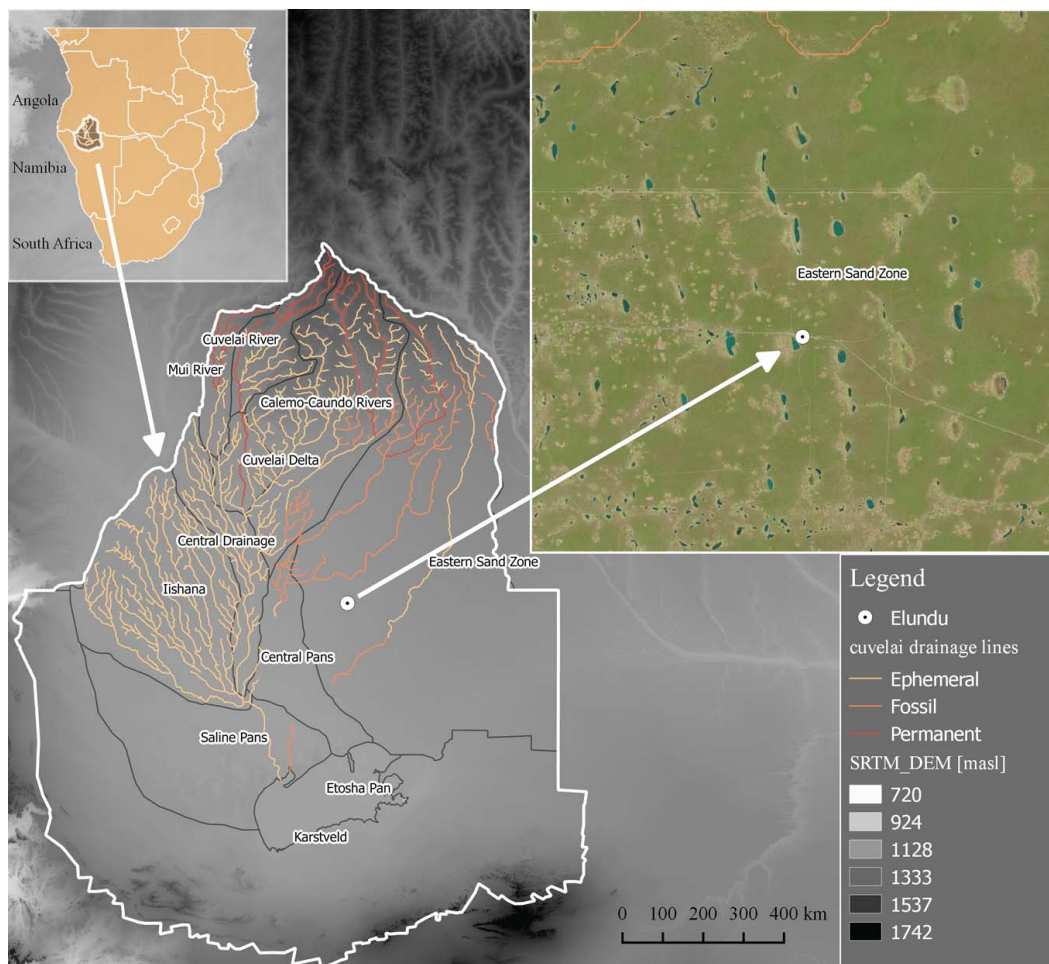
Figure 1. The study area is located in the northern part of the Cuvelai–Etosha Basin (CEB), which is subdivided by the political border between Angola and Namibia (left). Sampling was conducted in Elundu, located in the center of the CEB (center, right).

The investigated site is forested, predominantly vegetated with *Combretum collinum*, *Acacia erioloba*, and *Baikiaea plurijuga*. The deep Kalahari sand can reach a depth of over 40 m and has high saturated hydraulic conductivity (2.3–2.4 m day^{-1}) determined with double-ring infiltration experiments, high porosity (0.4), and low field capacity ($\sim 3.5\%$). Sampling and measurements were conducted during two field campaigns. The first field campaign was carried out between 9 and 15 June 2014 and the second between 15 and 22 November 2014. To determine heterogeneity of infiltration and evaporation processes and to evaluate an in situ approach determining stable isotopes in soil water nine plots within an area of 9000 m^2 were investigated. During the first campaign soil gas probes were installed at depths of 2, 5, 10, 15, 20, 25, 30, 40, and 50 cm. Two plots were established with different vegetation characteristics such that one was vegetated with shrubs and the other was exposed without any vegetation. During the second field campaign, probes were installed at depths of 2, 5, 7.5, 10, 12.5, 15, 17.5, 20, 25, 30, 40, 50, 60, 70, 80, 90, and 100 cm to reach a maximum resolution, es-

pecially for the top layer. Soil moisture measurements were conducted with a time domain reflectometry system (TDR, EasyTest, Poland) at the beginning of each measurement cycle with the same resolution. In addition to the in situ measurements samples were collected in headspace glass vials, crimp-sealed to avoid evaporation, and the soil water was extracted in the laboratory. Samples were transported via aircraft to the laboratory of the Federal Institute of Geosciences and Natural Resources (BGR) in Hanover, Germany.

In the laboratory, grain size analyses were conducted on 10 g of soil material from the extracted soil samples with the method proposed by Altuhafi et al. (2013). Soil water was extracted cryogenically using a slightly modified cryogenic-vacuum extraction method described by Koeniger et al. (2011). A custom-built isolated aluminum block is heated to 105 °C instead of a water bath. The sample vials are inserted into the hot aluminum block to evaporate the water sample. Each sample was evacuated at −3 mbar vacuum and extracted for 15 min. The extracted water samples were subsequently measured with a cavity ring-down spectrome-
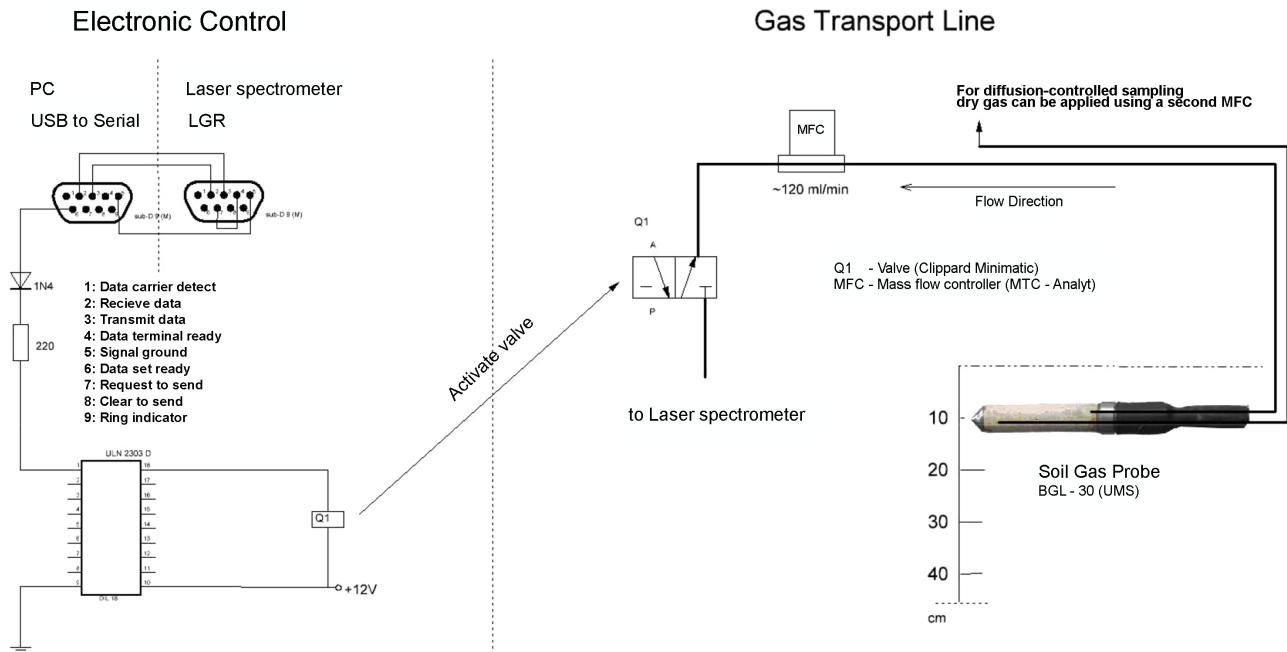
Figure 2. Gas transport (right) is controlled by an automated electronic control (left). The PC mimics the behavior of a laboratory autosampler communicating with the analyzer via a USB-to-serial adapter. High and low signals from the data set ready pin can be used to switch valves using an opto-isolator (ULN2303). Vapor is transported via the transport line from the soil gas probe to the ICOS device. The flow is measured with a mass flow controller (MFC).

ter (CRDS, model L2120-i, manufactured by Picarro Inc.). $^{18}O/^{16}O$ and $^2H/^1H$ isotope ratios are normalized on the international δ scale and expressed as parts per thousand:

$$\delta = \left[\left(\frac{R_{\text{sample}}}{R_{\text{reference}}} \right) - 1 \right], \qquad (1)$$

where R_{sample} $(-)$ denotes the $^{18}O/^{16}O$ isotope ratio (or $^2H/^1H$) of a water sample and R_{standard} $(-)$ those of the Vienna Standard Mean Ocean Water (VSMOW) (Coplen, 2011). All values where corrected for drift and memory applying the method proposed by van Geldern and Barth (2012). Precision for long-term quality check standards is better than 0.2 and 0.8 ‰ for water samples, but an additional error for sandy soils needs to be considered, which can be better than 0.8 and 4 ‰ for $\delta^{18}O$ and δ^2H, respectively, as suggested by Koeniger et al. (2011). The standard deviation determined from replicate samples (three per extracted soil sample) is used as an additional analytical error. Subscripts are used to distinguish between the in situ (I) and the cryogenically (C) derived isotope values in the remainder of the text.

For the determination of δ^2H_I and $\delta^{18}O_I$, commercially available soil gas probes (BGL-30, Umweltmesssysteme, Munich (UMS)) with a diameter of 9.4 mm and a length of 300 mm were connected to an integrated cavity off-axis liquid water isotope analyzer (OA-ICOS, Los Gatos Research, DLT100). This device does not measure continuously; each

measurement cylce is initiated by command that is sent by the analyzer via the Rs-232 interface. Thus it is mandatory to maintain the response, which is commonly done by the laboratory autosampler. Here it is done via the RS-232 interface of a laptop computer and a computer code that responds to the requests of the laser spectrometer (Fig. 2). Each soil gas probe is separated from the main transport line with a valve (Clippard Minimatic, USA). The valves are switched by a high or low signal from the data terminal ready (DTR) and request to send (RTS) pins of the modified USB-to-RS232 converter. A reduction in the electric tension output of the converter is necessary, which is done using a 220 Ω resistor. To protect the converter against inverse currents, a common diode is installed in reverse in front of the opto-isolator (ULN2303). The opto-isolator is necessary to eliminate voltage spikes from the +12 V power supply. To avoid over heating of the analyzer during daytime by direct solar radiation, a gazebo was positioned above the loading area of the pick-up truck where the analyzer is mounted. Power was supplied to the entire system using a common 230 V generator (single-phase 2.5 kW, gasoline, Schultz).

Four repeat measurements at each depth were performed during the first campaign. During the second campaign, six consecutive measurements were performed at each depth. A measurement cycle consisted of three steps: (i) a flushing phase where the cavity is evacuated, (ii) opening of a particular valve by the sample intake, and (iii) the measurement of

Table 1. Standards used for normalization, drift correction, and quality check. The standards are used for both the measurements with the in situ approach in the field and the extracted soil water in the laboratory.

Abbreviation	Description	δ^2H [‰]	σ	δ^{18}O [‰]	σ
HMER	Hanover sea water	−3.1	±0.4	−0.4	±0.13
HDES	Hanover distilled water	−55.9	±0.9	−8.12	±0.14
HLAU	Hanover Lauretaner water	−64.6	±0.6	−9.73	±0.10
HGLA	Hanover glacier water	−152.1	±0.9	−20.27	±0.11

Table 2. Values for HLAU (qc) with the corresponding standard deviation of their repetitive measurements (σ_{qc}), the mean standard deviation of the repetitive measurements of each measurement point (σ_{rep}), and the corresponding values of the cryogenic vacuum extraction (σ_{cry}) from the campaigns June/November 2014. Bare plots (B) and vegetated plots (V) were measured.

ID	Date	Init. time		δ^2H$_{qc}$ [‰]		σ_{qc}	σ_{rep}	σ_{cry}	δ^{18}O$_{qc}$ [‰]		σ_{qc}	σ_{rep}	σ_{cry}
E1.1	04.06.2014	09:30:00	B	−60.09	±	5.13	1.4	3.7	−10.04	±	0.66	0.7	0.8
E1.2	04.06.2014	15:30:00	V	−74.96	±	2.83	3	3.5	−13.16	±	0.01	0.6	0.6
					±	3.98	2.2	3.6		±	0.34	0.65	0.70
E2.1	15.11.2014	10:50:00	B	−73.25	±	0.87	1.17		−10.38	±	0.34	0.45	
E2.2	16.11.2014	08:00:00	B	−69.83	±	0.99	1.26		−8.05	±	0.48	0.35	
E2.3	16.11.2014	13:30:00	V	−71.11	±	0.49	2.21		−10.29	±	0.14	0.54	
E2.4	17.11.2014	11:00:00	V	−57.51	±	4.11	1.72		−8.45	±	0.14	0.28	
E2.5	18.11.2014	11:00:00	V	−64.82	±	1.86	1.52		−7.73	±	0.34	0.28	
E2.6	19.11.2014	07:30:00	B	−75.62	±	1.84	2.49		−6.81	±	0.81	0.5	
E2.7	19.11.2014	14:00:00	B	−79.35	±	1.27	1.93	3.5	−11.62	±	0.36	0.45	0.45
E2.8	20.11.2014	11:30:00	V	−25.24	±	2.53	1.45		−3.68	±	0.25	0.24	
E2.9	21.11.2014	11:30:00	V	−23.00	±	17.17	1.74		−15.59	±	4.17	0.37	
						2.15	1.86	3.57			0.36	0.46	0.62

the sample. Flushing introduces a vacuum of 0.1 Torr or less. The sample intake is controlled by valves which are opened for 10 s for each measurement while allowing a volumetric flow rate between 95 and 110 mL min^{-1}. The transported gas volume is measured with a flow rate measurement device (Analyt-MTC, 0–200 mL min^{-1}). The probe and the transport lines to the analyzer have a volume of approximately 40 mL. The sample lines are made of steel and are connected with Swagelok® connectors. After six consecutive measurements at one depth, the sampled soil volume is approximately 120 mL. Assuming that the soil volume around the 300 mm long probe is sampled equally over the whole length, a diameter of 1 cm around the probe will be directly affected by the uptake of vapor via the probe. Hence, the top layer is measured with reasonable resolution for this particular setup. The measurement of a 1 m deep profile considering 16 different depths with six repetitions and a resolution down to 2.5 cm for the top 20 cm takes about 4.5 h. The OA-ICOS device needs an additional warm-up of about 2 h in order to obtain reasonable precision.

During the second field campaign, three transects are measured consisting of three plots to characterize the spatiotemporal variability after two consecutive rain events. Each transect is 150 m apart, and three profiles are also taken per transect at a distance of 150 m from each other. Transects consist of bare plots as well as vegetated plots (Table 2). However, lateral roots could be found at each plot.

Standard preparation was done using 200 g of previously oven-dried (at 105 °C for at least 24 h) sandy substrate for each of the four standards (Table 2). The dried soil material was transported in aluminum bags (WEBA bags®, Weber Packaging GmbH, Güglingen, Germany) from the laboratory of the University of Windhoek to the field site and was then spiked directly in the field with 5 mL of water of known isotopic composition (Table 1) before the experiment commenced on the day of measurement. Normalization to the international scale is done using one low standard (HGLA) and one high standard (HMER). In addition, one standard for drift correction (HDES) and a quality check standard (HLAU) were used. The quality check standard is a water of known isotopic composition that is treated as an unknown sample. The difference between the known value of HLAU and the measured isotope value of HLAU expresses the measurement trueness of the system (Barwick and Prichard, 2011). All standards were measured at the beginning of each experimental sequence; additionally HDES and HLAU were measured at the end of each sequence. Isotope values of the standards used are illustrated in Table 1. The standards were used only for two consecutive measurement series and then new standards were prepared. Calibra-

tion standards were kept in flasks with a diameter of 2 cm and a length of 50 cm, in which the soil gas probes were stored and sealed to avoid evaporation.

Soil water balance

Recharge rates were determined in millimeters per year using a simple empirical relationship applied to the data of the deep isotope depth profile (> 4 m). Therefore, the difference between the deuterium excess of the local meteoric water line (LMWL) and the intercept of the linear regression to isotope data of deep soil water is defined as $\delta^2 H_{shift}$. This relationship is proposed by Allison et al. (1984) and for $\delta^2 H$ and $\delta^{18} O$ given here as in Clark and Fritz (1997):

$$R = \left[\frac{22}{\delta^2 H_{shift}}\right]^2 \tag{2}$$

and

$$R = \left[\frac{3}{\delta^{18} O_{shift}}\right]^2, \tag{3}$$

Assuming steady state, soil evaporation is calculated from the isotope depth profiles using an analytical solution (Allison et al., 1984).

$$E = (1 - h_a) N_{sat} \tau D^V \frac{(p - \theta_v)}{\rho z_{ef}} \tag{4}$$

Thus, evaporation can be determined providing the relative humidity h_a [−], the saturated water vapor pressure $N_{sat}[P]$ the tortuosity with $\tau = 0.67$ [−], the diffusivity of water vapor in air $D^V = 24 \times 10^{-6}$ [a], the density of water ρ [$M L^{-3}$], the porosity p [−], and the soil water content θ_v [$L^3 L^{-3}$]. Calculations were conducted for a mean ambient temperature of 20 °C and 50 % relative air humidity and further with 27 °C and 60 % for campaign 1 and 2, respectively. The depth of the evaporation front z_{ef} [L] can be determined by an exponential fit to the isotope depth profiles (Allison et al., 1985).

$$\delta = \delta_{res} (\delta_{ef} - \delta_{res}) \exp^{-z/z_{ef}} \tag{5}$$

The data of the isotope depth profile δ are calculated from the fitted parameters z_{ef} the isotope value of the reservoir δ_{res} and the isotope ratio at the evaporating front δ_{ef}. This will give a quantitative estimation of the soil water balance based on the presented isotope data. In addition, z_{ef} is determined from the grain size distribution as follows (Or et al., 2013):

$$z_{ef} = \frac{2\alpha}{\rho g} \left(\frac{1}{r^1} - \frac{1}{r^2}\right), \tag{6}$$

where $\alpha[M T^{-2}]$ is the surface tension of water calculated at 24 °C, g is gravitational acceleration, and r^1 [L] and r^2 [L] are the minimum and maximum grain size of the soil, respectively.

3 Results

3.1 Campaign 1

The first field campaign was conducted shortly after the rainy season (June 2014). No rain occurred during the campaign. The texture (medium sand) was uniform throughout the depth profile. No changes in texture were observed for the other investigated plots. Temperature and humidity variability within the sampling period between daytime (~ 30 °C_{max} and 15 %$_{min}$) and nighttime (~ 9 °C_{min} and ~ 90 %$_{max}$) was high during the first campaign.

During the first campaign (15 June 2014), measurements were taken at two plots (E1.1, E1.2) at a distance of 25 m apart on the same day. The measurement at E1.1 started at 09:30 and at 16:00 for plot E1.2. Plot E1.1 was not vegetated and had a thin soil crust in the top centimeter. Volumetric water content increased from 0.3 % at the top to 4.1 % at 50 cm depth (Fig. 3, left). Plot E1.2 was vegetated; a dense root mat was visible in the upper 10 cm. In contrast to E1.1, water contents were much lower, increasing from 0.3 % at the surface to 0.7 % at 50 cm depth (Fig. 3, center). The isotope depth profiles were of similar shape and magnitude for both profiles, with a maximum at 10 cm and an exponential decline down to the maximum depth. Due to low water contents in the upper 15 cm of the vegetated plot, not enough water could be extracted with the cryogenic extraction method. However, at 10 cm depth the same pattern as for profile E1.1 could be observed. The shapes of the isotope depth profiles were different for $\delta^{18} O$ and $\delta^2 H$ within the upper 5 to 10 cm. For instance, the maximum isotope values of $\delta^2 H_c$ and $\delta^{18} O_c$ were at 15 cm. In contrast, the maximum isotope values of $\delta^2 H_i$ and $\delta^{18} O_i$ were at 10 cm.

As depicted in Fig. 4, the deuterium excess for both profiles showed a maximum at 10 cm depth and exponentially declines down to 50 cm. At the vegetated plot, deuterium excess values were positive within the top 7.5 cm. Comparing deuterium excess values of the cryogenic extraction with those from the in situ measurements, it could be found that they agree well for the bare soil plot, but not at 10 and 15 cm depth. In contrast, all values measured in the field below 10 cm of the vegetated plot, which had low water contents (< 1 %), were shifted towards more positive values, indicating less evaporative enrichment. In comparison to the isotope depth profiles the deuterium excess depth profile has its minima at 10 cm for both methods except profile E2.7.

3.2 Campaign 2

During the second campaign, variations in temperature and humidity were much smaller compared to Campaign 1 (daytime ~ 35 °C_{max} and 30 %RH_{min}; nighttime ~ 20 °C_{min} and ~ 90 %RH_{max}). Two rainfall events were recorded (12 November 2014: 12 mm in the morning; 13 November 2014, 30 mm in the morning) at the climate station in Eenhana,
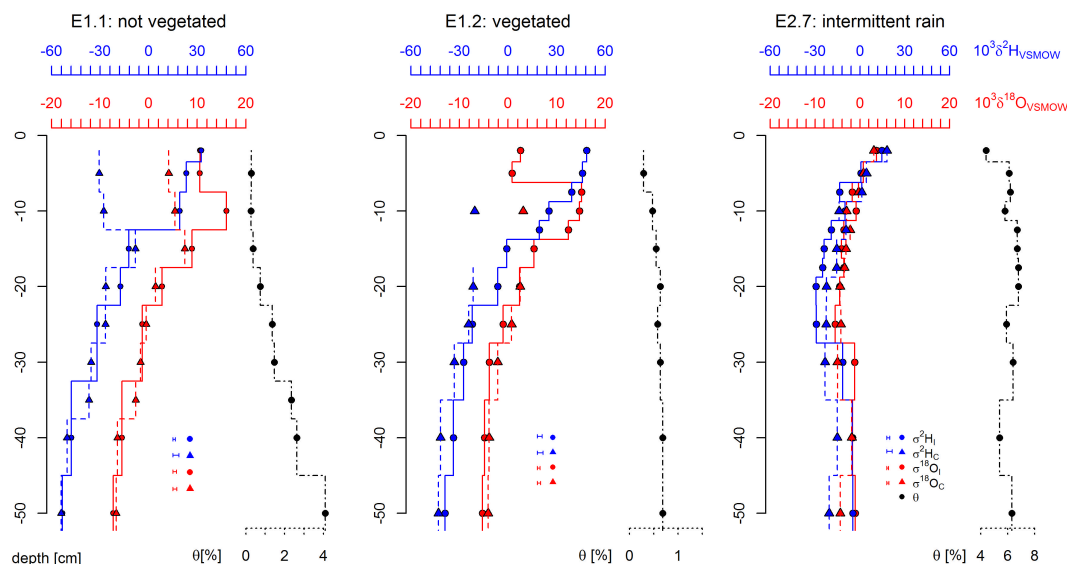
Figure 3. Depths profiles of the field campaign in June 2014 (E1.1, E1.2) and the field campaign in November 2014 (E2.7). Compared are isotope depth profiles extracted with the cryogenic vacuum extraction (dashed lines, triangles) and measured in situ (solid lines, dots). δ^2H is given in blue and δ^{18}O is given in red. Soil moisture is illustrated on the right of each plot (black). Standard deviation for each plot and each method is indicated by error bars in the legend of the plot.
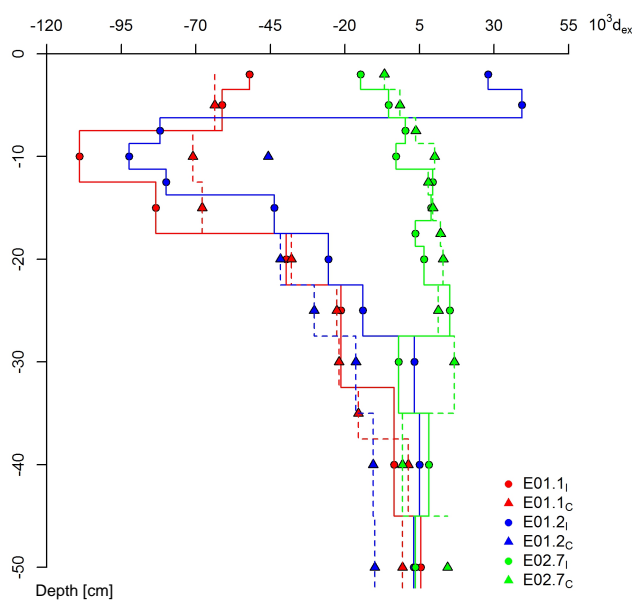

Figure 4. Deuterium excess for profiles E01.1 and E01.2 sampled in June 2014 and E02.7 sampled in November 2014. Compared are values from the cryogenic vacuum extraction (triangles) and the in situ measurements (circles).

which is approximately 15 km west of the experimental site. However, no isotope data were available until 17 November 2014. Later on during the campaign, a small rain event (16 mm) was sampled for isotopes on 17 November 2014 at 08:00 with −0.6 and 3.0 ‰ for δ^{18}O and δ^2H, respectively.

A smaller event (4 mm) was also sampled on 19 November 2014 with isotope values of 3.6 and 28.8 ‰ for δ^{18}O and δ^2H, respectively.

The plots that were sampled in November (rainy season) have higher water contents compared to those of the first campaign. One non-vegetated plot of the second campaign (E2.7; see Fig. 4, right-hand side, and Table 2) is used to compare the in situ and the laboratory results as an example with higher water contents. The water contents range between 4.4 and 6.8 %, with maximum values between 12.5 and 25 cm (Fig. 3, right). Strongest enrichment of δ^{18}O is in the top layer, declining exponentially with depth for both methods. There is good agreement between δ^{18}O$_I$ and δ^{18}O$_C$ except for depths at 30 and 50 cm. In contrast, there are substantial differences between δ^2H$_I$ and δ^2H$_C$. Above 25 cm, values of δ^2H$_C$ are higher (−15.5 to −22.6 ‰) than for δ^2H$_I$ (−25.0 to −29.2 ‰) and, conversely, lower below 25 cm with −23.4 to −15.2 ‰ for δ^2H$_C$ and −11.6 to −5.1 ‰ for δ^2H$_I$, respectively.

The agreement between in situ and cryogenically obtained isotope measurements is expressed with the root mean square error (RMSE). There is good agreement between in situ and cryogenically obtained isotope measurements for both isotope depth profiles of the first campaign between 15 and 50 cm (RMSE = 3.9 and 9.2 ‰ for δ^{18}O and δ^2H, respectively). However, higher values were observed for the in situ approach at shallower depth (RMSE = 7.0 and 43.4 ‰ for δ^{18}O and δ^2H, respectively). In general, better agreement can be observed for δ^{18}O compared to δ^2H values. Both isotope profiles of the first campaign derived from the cryogenic vacuum extraction show a maximum at 15 cm with an exponen-

tial decline down to depth. Values of the in situ measurement show this maximum at 10 cm, but only for $\delta^{18}O_I$. The profile of the second campaign shows good agreement within the top 25 cm for $\delta^{18}O_I$ but for δ^2H only within the upper 10 cm. In terms of measurement trueness for the set of these three profiles we obtain 6.86 and 1.87 ‰ for δ^2H_I and $\delta^{18}O_I$, respectively.

A list of the quality check standards for δ^2H_{qc} and $\delta^{18}O_{qc}$ of the two campaigns is shown in Table 2. The standard deviation of the repetitive measurements for each depth is a measure of measurement precision. After drift correction and normalization of the isotope depth profile E1.1 the precision (σ_{qc}) of the quality check standard (HLAU) was 5.1 ‰ δ^2H and 0.66 ‰ $\delta^{18}O$, respectively. The mean precision of the repetitive measurements (σ_{rep}) is 2 times better for δ^2H_I than for the precision of the repetitive measurements (σ_{cry}) for values derived from the cryogenic vacuum extraction δ^2H_C. Values of $\delta^{18}O_{qc}$ show higher similarity (refer to Table 2). The measurement of the second profile E1.2 is less precise for δ^2H_I but in the same range as δ^2H_C. Similar precision as for profile E1.1 is found for the third profile, E2.7, for both δ^2H and $\delta^{18}O$.

3.3 $\delta^{18}O$ vs. δ^2H

In Fig. 5 the $\delta^{18}O$ to δ^2H relationship is shown. The LMWL is derived from historical data collected in the CEB and has a slope of 7.3 ($R^2 = 0.96$). Additionally, mean values of local groundwater ($\sigma^{18}O = 0.91$, $\sigma^2H = 4.27$) and soil water down to a depth of 4 m with 10 cm resolution are presented. Soil water from the first field campaign derived from the cryogenic vacuum extraction plots along an evaporation line with a slope of 2.4 ($R^2 = 0.79$) for the non-vegetated plot and 3.1 ($R^2 = 0.96$) for the vegetated plot. In situ measurements of the non-vegetated plot have a slope of 3.9 ($R^2 = 0.84$). With the first 10 cm of the unvegetated profile excluded, the slope is 2.9 ($R^2 = 0.73$). Values of the vegetated site derived from the in situ measurements have a slope of 3.0 ($R = 0.46$) and are shifted towards more positive δ^2H values. With the top 15 cm of the in situ measurement excluded, the slope remains the same but R^2 increases to 0.9. Values from the second campaign show a much higher slope, with 5.3 ($R^2 = 0.75$) for the in situ measurement and 5.1 ($R^2 = 0.96$) for the cryogenic vacuum extraction, and plot close to the LMWL.

3.4 Spatiotemporal variability

Each profile of the second campaign is measured at 18 different depths and each depth with six repetitions. After drift correction of the isotope data, the mean precision considering the quality check measurements (σ_{qc}) for more than 140 measurement points is 2.15 ‰ for δ^2H_I and 0.36 ‰ for $\delta^{18}O_I$ (Table 2). Mean standard deviation of the repetitive measurements (σ_{rep}) of each depth is 1.86 ‰ for δ^2H_I and 0.46 ‰ for $\delta^{18}O_I$, respectively. As shown in Table 2, the mean stan-

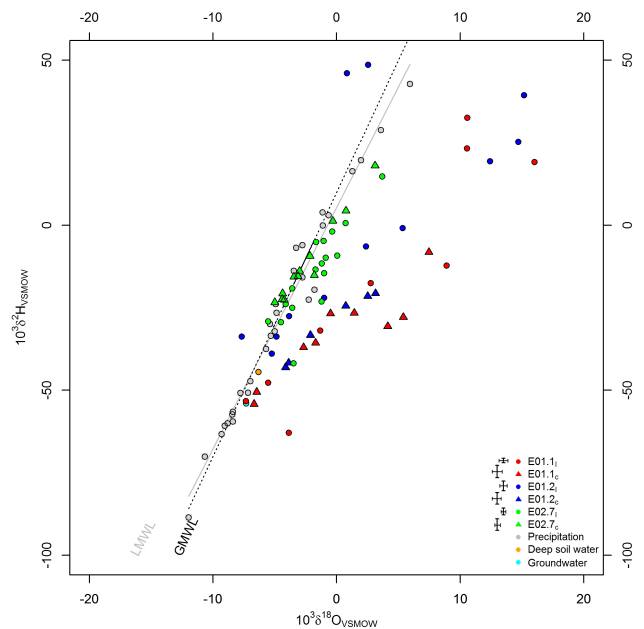**Figure 5.** $\delta^{18}O$ vs. δ^2H plot of the profiles E01.1, E01.2, E02.7. Further shown is the local meteoric water line (LMWL) for the northern part of Namibia as well as the global meteoric water line (GMWL). A mean value of shallow groundwater is plotted, as well as soil water of a depth profile down to a depth of 4 m.

dard deviations of the repetitive measurements are similar to those derived from the quality check standard. Differences are observed between σ_{qc} and σ_{rep}. However, the precision of δ^2H is within the range of the mean measurement trueness of 5.4 ‰ . The measurement trueness of $\delta^{18}O$ is much higher with 0.11 ‰. There are two outliers (E2.8, E2.9) which were not considered for the mean precision.

Mean values of each transect are shown to illustrate an averaged temporal characteristic with intermittent rainfall (Fig. 6) for this particular area; both rain events are indicated by a grey dot on the x axis. The first transect is affected only by the first set of rain events (E2.1 to E2.3) and was measured within two consecutive days. The next transect (E2.4 to E2.6) is affected by the 16 mm event (17 November 2014), for which isotope data are available and the profiles were measured in a period of 3 days. Finally, the last three plots (E2.7 to E2.9) showed most evaporative enrichment and only experienced additional precipitation (4 mm) on 19 November 2014. Maximum infiltration depth varied between 65 and 95 cm. Water content varied between 0.5 and 9.5 %. From comparison of the three transects it can be observed that the variability in isotope depth profiles decreases from the first to the last transect and an evaporation profile develops.

To account for spatial variability, mean values of soil moisture were calculated for each depth of the nine plots. Additionally, the standard deviation of each depth for soil moisture, $\delta^{18}O$ and δ^2H are calculated. Fig. 7 shows mean soil
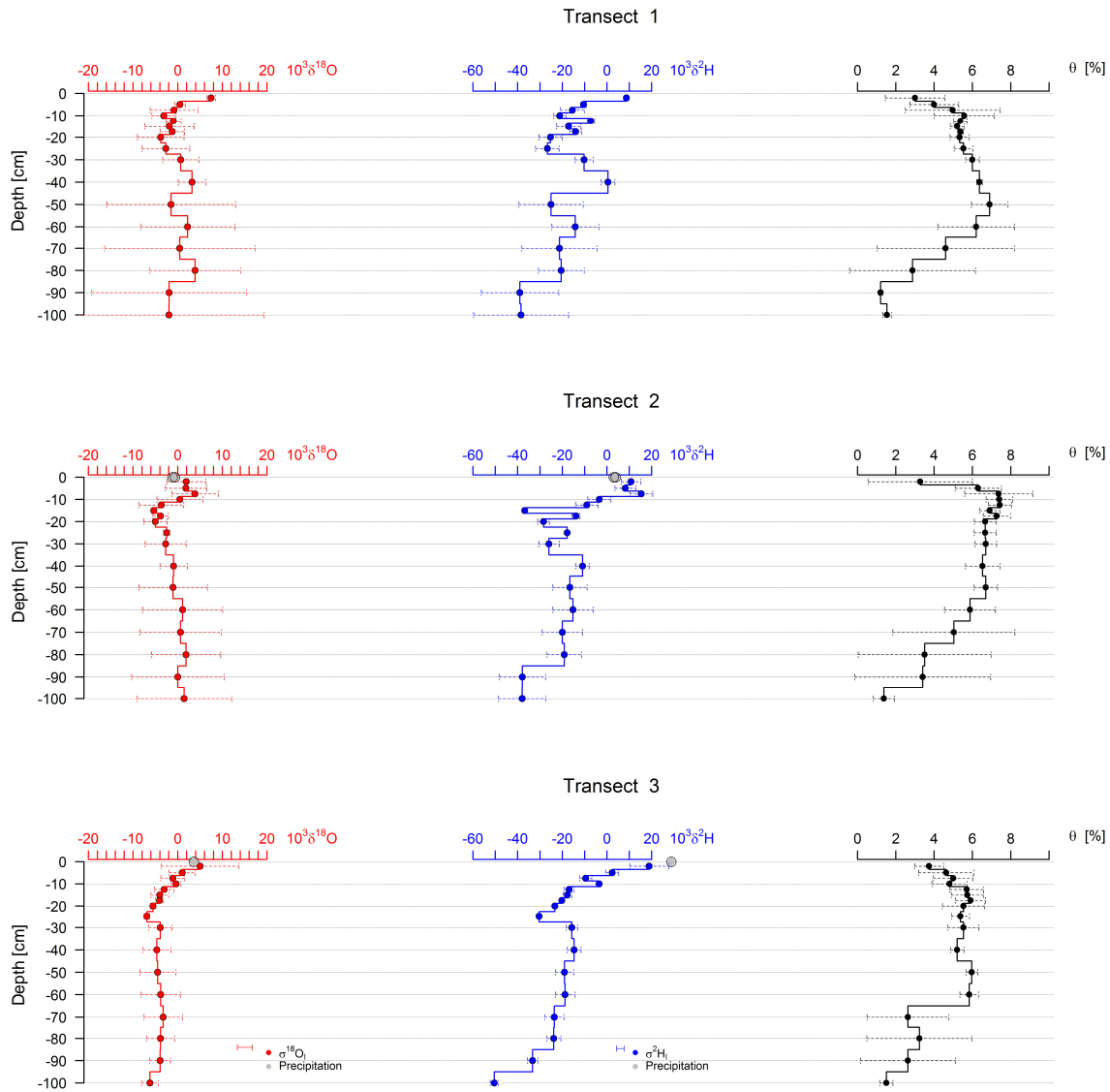
Figure 6. ^{18}O (red), ^{2}H (blue), and soil moisture (black) depth profiles. Shown are mean values for three transects consisting of three single profiles derived from in situ measurements. Mean standard deviation σ of all quality check standards (qc) is shown in the legend. Rainfall isotope values are indicated on the x axes in grey.
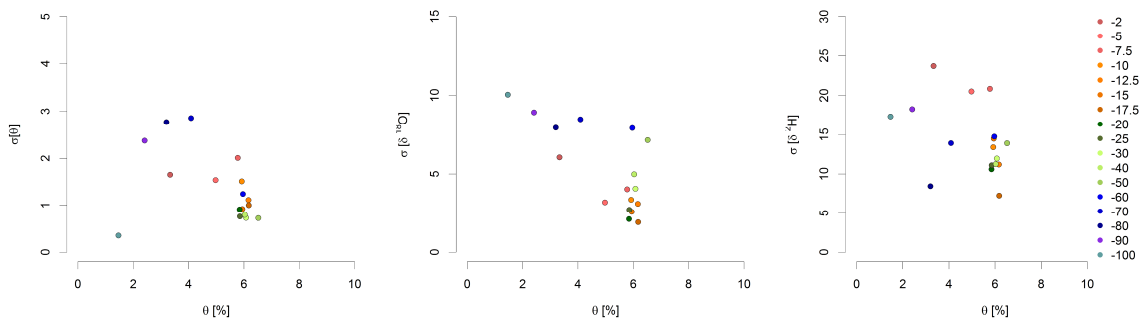

Figure 7. Mean soil moisture (Φ) for each depth plotted against the standard deviation of soil moisture $\sigma[\Phi]$ between each depth as well as standard deviation of $\sigma[\delta^{18}O]$ and $\sigma[\delta^{2}H]$.

Table 3. Soil evaporation (E) is derived from stable isotope depth profiles. The isotope value of the reservoir δ_{res}, the evaporating front δ_{ef}, and the effective depth z_{ef} are estimated from an exponential fit to the isotope depth profiles. The soil water storage (S) is calculated from the soil moisture depth profile. Transpiration (T) is the remainder from annual precipitation ($P = 660$ mm) after subtracting the recharge ($R = 4$ and 5 mm for ^{2}H and ^{18}O, respectively), E, and S. The partitioning between soil evaporation to transpiration is calculated as the contribution of transpiration (T/ET) to evapotranspiration (ET) for a range of soil moisture conditions Θ.

		z_{ef} [mm]	δ_{res} [‰]	δ_{ef} [‰]	E [mm yr^{-1}]		S [mm]	T [mm yr^{-1}]		T/ET [%]	
					$\Theta : 1\%$	$\Theta : 7\%$		$\Theta : 1\%$	$\Theta : 7\%$	$\Theta : 1\%$	$\Theta : 7\%$
	Cryo										
	bare	155	−48.2	31.4	147	125	40	468	490	76	80
	vegetated	127	−5.2	32.5	179	151	9.5	467	495	72	77
^{18}O	wet	79	−4.8	5.4	349	295	122	184	238	35	45
	In situ										
	bare	115	−6.4	46	197	167	40	418	448	68	73
	vegetated	139	−7.4	34.6	164	139	9.5	482	507	75	78
	wet	86	−5.8	5.9	321	271	122	212	262	40	49
	Cryo										
	bare	388	−84.1	21.8	59	49	40	557	567	90	92
	vegetated	364	−62.9	8.5	62	53	9.5	585	594	90	92
^{2}H	wet	90	−26	28.7	307	259	122	227	275	43	51
	In situ										
	bare	225	−65	49	101	86	40	515	530	84	86
	vegetated	174	−42	69	131	111	9.5	516	536	80	83
	wet	82	−32.8	27	336	285	122	198	249	37	47

moisture of each depth against the standard deviation of soil moisture and those of the two isotopes. Basically, high ($> 4\%$) and low ($< 2\%$) water content have lower variability in soil moisture compared to intermediate values. In contrast, the standard deviation of δ^{18}O and δ^2H increases with decreasing soil water content.

3.5 Soil water balance

Precipitation (P) for the rainy season was measured with an amount of 660 mm. Recharge estimated from soil water stable isotope data is less than 1 % of precipitation. It ranges between $R = 4$ and 5 mm yr^{-1} derived from $\delta^2 H_{shift}$ and $\delta^{18}O_{shift}$, respectively. The soil water storage (S) is derived from the soil moisture depth profile and the evaporation front is determined from the exponential fit to the water stable isotope depth profiles. Results are summarized in Table 3. Soil evaporation (E) is determined from z_{ef} using the isotope depth profiles. The mean of all results from E1.1 and E1.2 is 120 ± 50 mm yr^{-1}. Then, recharge (R), soil water storage (S), and soil evaporation (E) are subtracted from precipitation (P). The remainder is potentially available for transpiration (T) with 510 ± 50 mm yr^{-1}. Runoff can be neglected because it was not observed at the experimental site. Hence, the contribution of transpiration to total evapotranspiration (T/ET) is 81 ± 7 %. The potential contribution of transpiration (T/ET) or root water uptake at the non-vegetated plot is

between 76 and 92 %. At the site underneath the canopy and vegetated with shrubs, (T/ET) is between 72 and 92 %.

Values of z_{ef} range between 110 and 290 mm, which is in agreement with values derived from a physical model proposed by Or et al. (2013). Considering two different ranges, one for finer and one for coarser textures, we derive a depth z_{ef} of 210 mm and 118 mm for $r^1 = 63$–112 µm and $r^2 = 630$–1120 µm, respectively. Using these values to calculate E for profiles from June 2014 we derive values between 67 and 79 mm yr^{-1} and 161 and 201 mm yr^{-1} for r^1 and r^2, respectively.

After the rain events during the second field campaign the evapotranspiration pattern is dominated by soil evaporation. The evaporation front is still developing ($z_{ef} = 82$–90 mm) and T/ET is much lower at 35–51 %. With this methodology applied to the different transects, E decreases from 4 to below 1 mm day^{-1} (not shown).

4 Discussion

The potential to determine stable isotopes of soil water indirectly by measuring the vapor from the pore space directly in the field were able to be demonstrated through use of a liquid water analyzer. Results show that the precision of the in situ approach is better than 0.8 and 2.5 ‰ for δ^{18}O and δ^2H, respectively. This is a feasible precision when compared to the precision of isotope values obtained from the cryogenic vac-

uum extraction method, which are 0.8 and 3.5 ‰ for $\delta^{18}O$ and δ^2H, respectively. It is still worse compared to the precision that can be achieved measuring stable isotopes directly from water samples (0.2 and 0.8 ‰ for $\delta^{18}O$ and δ^2H). However, it needs to be considered that such laser spectrometers are in general situated in a temperature-controlled laboratory. In this study, measurement trueness and precision of the presented in situ system is mainly limited by the environmental conditions. If the laser spectrometer and the autosampler were operated within a temperature-controlled environment, the precision could possibly be improved. However, this study could demonstrate that it is possible to determine stable isotopes of soil water directly in the field with a similar or even better precision compared to destructive sampling and a subsequent soil water extraction in the laboratory. This creates possibilities to investigate water vapor transport processes that are difficult to measure with other techniques such as soil moisture or suction tension measurements. Evaporation processes are physically well described (i.e., Or et al., 2013), but their determination in the field remains difficult. An approach to observe evaporation was presented by Rothfuss et al. (2015), who were able show the development of an isotope depth profile in a drying soil column experiment with a similar in situ approach as in the present study. However, their experimental setup did not reflect conditions that can be found at our study site, since much higher temperature and humidity gradients were observed between day and night.

4.1 Campaign 1

Results of the first field campaign demonstrate good agreement of the isotope depth profiles between the cryogenic vacuum extraction method and the in situ approach for deeper parts of the soil profile, as well as a divergence in the top 15 cm. Differences could be a result of an incomplete soil water extraction, Rayleigh fractionation caused by the uptake of air from the in situ measurement, natural processes, or natural heterogeneity.

An incomplete extraction of water will result in depleted isotope values of the extracted soil water. However, this is unlikely for fine sand with low water holding capacity and low abundance of silt and clay. The cryogenic vacuum extraction is adequate to completely extract the water in sandy soils (Koeniger et al., 2011). Hence, the extracted soil water isotopic composition will reflect the "true" isotope values of the pore water.

Measuring soil water vapor or atmospheric vapor using the soil gas probe in a coarse material can lead to a mixed sample. However, the extracted air volume is low and a divergence of isotope values is only visible within the top 15 cm of the dry profiles (Fig. 3, left and center). Evaporative enrichment is reflected in the deuterium excess (d_{ex}) and also in the so-called evaporation line (Craig and Gordon, 1965). Evaporative enrichment could also be enhanced by the uptake of water vapor through the measurement (Figs. 5 and 6).

The equilibrium condition prevailing between soil liquid and gas phases is disturbed when water vapor is removed, causing the sampled water vapor to be depleted at the first stage. After some time, depending on the uptake rate and the soil water content, the initial isotope values of the remaining soil water may become higher; this will be reflected in the isotope values of the sampled gas and generally may be a cause of reduced precision. However, enrichment caused by the uptake of air through the measurement is not visible for deeper parts of profile E1.2, which is dry as well. Hence, the argument that low water contents would advocate showing higher isotope values for deeper parts of the vegetated profile would be consistent. This is not observed at the vegetated plot, where soil water contents are below 1 % throughout the whole profile (Fig. 3, center). Since the in situ approach is based on the same principle as the equilibration bag method, its applicability on samples with low water content is supported by a recent study of Hendry et al. (2015), who found that the measurement accuracy of their equilibration procedure could be improved by increasing the sample amount of low water content soils to increase the amount of water available for equilibration in the bag.

It should be noted that destructive sampling was conducted one day after the in situ measurements because it was assumed that the isotope profiles are in steady state (Barnes and Allison, 1988), and the experimental setup did not allow for simultaneous sampling. Therefore, the observed differences in the upper part of the soil profile might rather be attributed to kinetic processes, because vapor transport (i.e., evaporation) and hence isotopic enrichment will be more pronounced at shallow depths as described by Braud et al. (2009). Natural temporal variability such as high temperature and humidity changes between day and night could be another possible explanation. During the day evaporation dries the top layer due to vapor transport into the atmosphere. During the night, temperatures decrease and relative humidity increases. Low soil water contents and a back diffusion of vapor into the upper part of the soil can cause condensation or adsorption (Agam and Berliner, 2006), affect isotope values (Rothfuss et al., 2015), and significantly increase soil water content (Henschel and Seely, 2008). This might deplete isotope values of the remaining soil water within that upper layer. It has already been shown in a numerical study that diurnal variations in evaporation can be large depending on the energy budget at the surface, but the influence on isotope concentrations needs further investigation, especially under field conditions (Braud et al., 2005).

Another possibility for a change in isotopic composition at shallow depths could be hydraulic lift. In this case, water from deeper soil layers with higher water potential can move through the root system to soil layers with lower water potential (Dawson et al., 1993). The dense mat of fine roots observed in the upper part of the soil profile, together with low water contents and the differences between the isotope depth profiles, could be an indicator for this process. However, the

measurement of soil physical properties, stable isotopes of soil water, and xylem covering the diurnal cycle would be necessary to distinguish between vapor back diffusion or hydraulic redistribution.

4.2 Campaign 2

In contrast to depth profiles of the first campaign, the rain-influenced profile E2.7 does not show such a divergence in the top layer as observed at E1.1 and E1.2. As shown in Fig. 5, the deuterium excess indicates that precipitation water is dominant. Good agreement is found in the top layer for both isotopologues. Mixing with atmospheric vapor might be negligible considering the high soil water contents. Destructive sampling was done directly before the in situ measurement started. It needs to be noted that in situ measurements at 10 cm depth were done 90 min after the destructive sampling was conducted, while in situ measurements at 30 cm depth were conducted even 120 min later. Differences can be caused by the time lag between destructive sampling and in situ measurements, vapor transport processes induced by temperature gradients, or diffusion.

Considering that humidity of the pore space is close to saturation under the present "wet" conditions, but also if the soil moisture is around wilting point, humidity of the pore space is close to saturation. Then temperature gradients will cause movement of vapor downward or upward depending on the temperature profiles (Abramova, 1969). Further, soil evaporation can be separated into direct evaporation from a water saturated surface (stage I evaporation) and diffusion-controlled vapor transport (stage II evaporation) (Or et al., 2013). Therefore, observed differences between δ^2H_I and δ^2H_C for profile E2.7 (Fig. 3, right) might be attributed to the exchange between the evaporation-depleted vapor that was transported from the deeper zone (30 to 50 cm) to shallower depths (12.5 and 25 cm) due to diffusion-controlled evaporation (stage II).

4.3 $\delta^{18}O$ vs. δ^2H

Values for in situ measurements and cryogenic extraction plot on evaporation lines which are similar in slope (excluding the top 12.5 cm). The outliers in the top-right area and those above the LMWL of the δ^2H vs. $\delta^{18}O$ plot (Fig. 5) are from the top 12.5 cm of the profiles. As discussed earlier, diurnal temperature and humidity cycles could cause not only condensation in the upper part of the soil profile but also higher enrichment during the daytime as compared to the conditions during the night, when the soil is colder than atmospheric vapor. Further, the interaction between soil water potential and water vapor might be driven by relative humidity (Wilson et al., 1997), but its effect on isotope fractionation is not well understood and will be a challenge for future research (Soderberg et al., 2012). The investigation of such processes using in situ approaches for stable isotope analysis

seem to be promising in this regard, since the composition of vapor can be measured in the field.

4.4 Spatiotemporal variability

The boundary conditions of the second field campaign caused quite a heterogeneous pattern with regard to both the development of the moisture front and the isotope depth profiles. Observations were made that showed how the infiltrating water developed under evaporation with light, intermittent rainfall events. This is reflected in both the shape of isotope depth profiles of the three transects and the standard deviations within one transect (Fig. 6). Other studies showed similar patterns in the context of a numerical experiment (Singleton et al., 2004). The first transect (Fig. 6, transect 1) has variable isotope values throughout the whole depth. The isotope depth profile of transect 1 shows maxima and minima of isotope values which appear to reflect a similar profile from a humid climate. This kind of layering is commonly used in humid regions to determine transit times of unsaturated zone water where precipitation has seasonality to its isotopic composition (Coplen et al., 2000; Lee et al., 2007). However, here, it is attributed to variations in rainfall composition and infiltration patterns on a much smaller timescale, generally daily. Zimmermann et al. (1967) described that isotopically distinct rain that is consecutively infiltrating into the soil will move downward, distinguishable by a boundary between older rainwater below and younger water above. Hence, the most depleted values found at 20 and 50 cm (Fig. 6, transect 1) might correspond to certain rain events which would not emerge from the soil moisture measurements alone. These depleted zones are not visible in the other transects, which are possibly overprinted by vapor transport processes and evaporation.

In the short time period after a precipitation event, the top part of the evaporation profile (transect 1) was considerably displaced as theoretically described by Allison et al. (1984). Variations in isotope values are attenuated with time by vapor phase redistribution (transect 2) (Fontes et al., 1986) and an evaporation profile begins to develop (transect 3) (Rothfuss et al., 2015). Further, it can be observed that infiltrating water of small, intermittent events compresses the isotope profile (Barnes and Allison, 1988; Singleton et al., 2004). Therefore, the presented in situ measurements have great potential to visualize theoretically discussed processes with feasible measurement trueness under natural field conditions.

Spatial variability in soil moisture is well known (Western et al., 2004). It can be expected that stable isotopes will also distribute heterogeneously within the unsaturated zone. The relationship between mean soil moisture and δ^2H does not allow for a resilient conclusion because of low measurement trueness in this study. However, it appears that it behaves differently for δ^2H and $\delta^{18}O$ values when compared to soil moisture. The differences might be related to vapor diffusion processes or to biological processes. For instance,

Dawson et al. (2002) discussed the isotopic composition of different carbon and water pools. Soil respired (CO$_2$) will equilibrate with the abundant soil water and might cause additional changes to the isotopic composition of the soil pore water.

4.5 Soil water balance

The soil water balance is calculated from isotope depth profiles. The presented results are in agreement with other isotope-based partitioning studies. Those studies suggest a contribution of transpiration of more than 70 % to the total evapotranspiration flux as Sutanto et al. (2014) discussed in a recent review. In addition, the findings from the first field campaign showed that the development of the evaporation profiles appeared to be independent of leaf/vegetation cover. Based on the data and calculations of this study, it seems that soil cover might be of minor importance for long-term soil evaporation quantities.

Differences between the two sites of the first field campaign are minimal regarding the shape of the isotope depth profiles. In addition, the evaporating front and the calculated evaporation rates using Eqs. (4 and 5) are similar for both sites. Because of the litter layer and the shaded nature of plot E1.2 it could be expected that less evaporation takes place and hence less enrichment and a lower deuterium excess would appear for the in situ measurement (Fig. 4). However, this is not visible and suggests humidity to be the main driver for isotopic enrichment as demonstrated in a numerical study by Braud et al. (2005).

4.6 Potential limitations

Water vapor mixing ratio dependencies (Wang et al., 2009; Sturm and Knohl, 2010; Rambo et al., 2011; Aemisegger et al., 2012) are of minor importance in this study, because the water content was maintained within the density of approximately $2-4 \times 10^{16}$ molecules cm^{-3} as recommended by Los Gatos Research. It is assumed that small variations will be reflected in the standard deviation of the measurements. Additionally, inference through organic contamination is neglected in this study. However, if necessary to account for inference, recent efforts include calibration strategies in this regard (Wu et al., 2014). Possible fractionation due to high salt concentrations or chemical reactions as observed by Oerter et al. (2014) are negligible because the cation exchange capacity (CEC) of the sand was 0.5 meq 100 g^{-1} and total organic carbon (TOC) 0.22 %.

During the second field campaign, information on long-term precision and spatiotemporal variability was investigated. Comparison of the quality check standards of the two campaigns shows that the precision within one series (σ_{rep}) of δ^2H is one-third better than the long-term measurement trueness. However, the measurement trueness of δ^{18}O is 3 times greater than the mean precision (Table 2). This can

likely be improved by utilizing a more sophisticated technical setup, e.g., temperature-controlled conditions. Another reason could be the difference in the physical properties of the probe pores such as the diffusivity of gas (Merlivat, 1979). Though there are no detailed chemical data available, it is unlikely that chemical properties are responsible, since the sandy soil has a low CEC. More likely are biological processes that are introduced due to the sudden availability of water, such as enhanced soil respiration (Dawson et al., 2002). Nevertheless, there are no data (i.e CO$_2$ measurements) available to support this assumption. Therefore, it would be beneficial to measure CO$_2$ concentration in parallel. However, the precision appears to be sufficient to monitor processes of a diurnal timescale and also comparable to other systems that were tested in the field, e.g., Volkmann and Weiler et al. (2014) demonstrating precision values of 2.6 and 0.38 ‰ for δ^2H and δ^{18}O, respectively.

Condensation within the sample system can lead to unreliable data. This can be prevented by heating the sample lines, flushing the sample lines with dry air, or sufficient dilution of the sample. Thus, under conditions where the ambient temperature is significantly warmer than the soil temperature, a simple valve-controlled membrane inlet will be sufficient for an indirect determination of isotopes in unsaturated zone or saturated zone water. During the daytime this is the case at the presented study site, but this changes drastically overnight as described. Dilution of the vapor concentration can be done by providing dry gas at the other end of the available probes. In the case of pure diffusion sampling, the maximum dilution rate depends upon the absolute amount of water molecules in the vapor and is controlled by the length of the probe, their diffusion properties, the flow velocity, and the temperature at depth. The flow velocity can be different depending on the laser spectrometer that is used. Adding a mixing chamber at the head of the probe has the distinct advantage of additional mixing directly before the vapor enters the sample line (Volkmann and Weiler, 2014). This leads to independence of flow velocity, probe length, and membrane diffusion properties with regard to the water content of the sampled vapor. Under dry conditions it might be useful to increase the probe length, since the soil volume around the probe affected by the measurement will be reduced.

A critical point is the long-term application of membrane-based methods. The pore space of the probes can be altered over time, which might increase the memory effect of the system. Further, the calibration of the in situ methods of Volkmann and Weiler (2014) and this study used prior oven-dried substrate for calibration. This procedure assumes that all water is evaporated during oven drying and only the added standard water will be measured afterwards. The same assumption is made using the equilibration bag method if the standards are treated in the same way as described. However, interlayer water or adsorbed water of clay minerals is commonly removed under vacuum while heating the sample to 200 to 300 °C for several hours (VanDeVelde and Bowen,

2013). The adsorbed and interlayer water is bound to the mineral surface and exchanges with atmospheric water vapor within hours (Savinand and Epstein, 1970). Hence, for soils containing clay minerals, a calibration procedure using previously oven-dried soil materials might lead to insufficient data. The presented direct comparison of the cryogenic vacuum extraction with a membrane-based in situ measurement showed that this calibration procedure is at least applicable for fine sand. However, application of this calibration procedure to soil samples with finer texture will probably lead to insufficient data, especially if clay, silt, and/or salt contents are high (Oerter et al., 2014).

5   Conclusion

The present study demonstrates that high-resolution in situ sampling of stable isotopes in the unsaturated zone is feasible. Long-term measurement trueness within the presented campaigns is about 2 times lower for δ^2H and 3 times for δ^{18}O than for the short-term precision of each profile. This can possibly be improved through better temperature control of the analyzer or temperature-compensated devices if available. In situ measurements can be applied with minimal technical effort for remote applications. They further show good agreement with values derived from cryogenic soil water extractions. Differences between the two methods are predominantly within the given accuracies of the methods. Divergence in the upper soil layer between in situ and destructive sampling suggests enhanced soil–atmosphere interactions, kinetic processes due to high evaporation rates, or hydraulic redistribution. Evaporation induced by the measurement procedure might decrease the precision depending on the uptake rate and the soil water content. Low humidity in relation to soil water potential and isotope fractionation needs further investigation. However, more importantly, to prevent the collection of insufficient data when applying an in situ approach, one has to carefully consider the applied calibration procedure depending on the research question and the soil type. In addition, there is a trade-off between technical effort, control setup, probe type, environmental conditions, and costs. The presented and also other in situ measurement approaches have great potential for investigation of transient processes within the unsaturated zone. It was not possible to study this until field deployable laser spectrometers and in situ techniques became available. The determination of water stable isotopes in the unsaturated zone directly in the field allows for monitoring of transient processes which would not be possible with destructive sampling strategies. This creates new possibilities for the design of tracer experiments with water of a labeled isotopic composition as a conservative tracer. However, this is limited by the measurement frequency of the provided system, which is now at least able to capture diurnal processes with the presented vertical resolution. In addition, a much higher spatial resolution can be achieved with much lower time con-

sumption compared to conventional approaches. The proposed technique offers the possibility to investigate unsolved questions regarding soil–atmosphere interactions such as water vapor intrusion and transport plus effects of diurnal evaporation cycling on isotope depth profiles.

References

Abramova, M. M.: Movement of moisture as a liquid and vapor in soils of semi-deserts, Internat. Assoc. Sci. Hydrol., Proc. Wageningen Symposium, 83, 781–789, 1969.

Aemisegger, F., Sturm, P., Graf, P., Sodemann, H., Pfahl, S., Knohl, A., and Wernli, H.: Measuring variations of δ^{18}O and δ^2H in atmospheric water vapour using two commercial laser-based spectrometers: an instrument characterisation study, Atmos. Meas. Tech., 5, 1491–1511, doi:10.5194/amt-5-1491-2012, 2012.

Agam, N. and Berliner, P. R.: Dew formation and water vapor adsorption in semi-arid environments – A review, J. Arid Environ., 4, 572–590, doi:10.1016/j.jaridenv.2005.09.004, 2006.

Allison, G. B. and Hughes, M. W.: The use of natural tracers as indicators of soil-water movement in a temperate semi-arid region, J. Hydrol., 60, 157–173, 1983.

Allison G. B., Barnes, C. J., Hughes M. W., and Leaney, F. W.: Effect of climate and vegetation on oxygen-18 and deuterium profiles in soils, Int. Symp. Iso. Hydrol. Water Resour. Dev., Vienna, Austria, 105–123, 1984.

Allison G. B., Barnes, C. J., and Hughes M. W.: Estimation of evaporation from the normally "dry" lake frome in south Australia, J. Hydrol., 78, 229–242, 1985.

Allison, G. B., Colin-Kaczala A. F., and Fontes C. J.: Measurement of Isotopic Equilibrium between Water, Water Vapor and Soil CO2 in Arid Zone Soils, J. Hydrol., 95, 131–141, 1987.

Allison, G. B., Gee, G., and and Tyler, S. W.: Vadose-Zone Techniques for Estimating Groundwater recharge in Arid and Semiarid Regions, Soil Sci. Soc. Am. J., 58, 6–14, 1994.

Altuhafi, F., O'Sullivan, C., and Cavarretta, I.: Analysis of an Image-Based Method to Quantify the Size and Shape of Sand Particles, J. Geotech. Geoenvironal, 139, 1290–1307, doi:10.1061/(ASCE)GT.1943-5606.0000855, 2013.

Barnes, C. J. and Allison, G. B.: Tracing of Water Movement in the unsaturated zone using stable isotopes of hydrogen and oxygen, J. Hydrol., 100, 143–176, 1988.

Barwick, V. and Prichard, E.: Terminology in Analytical Measurement: Introduction to VIM 3, Eurachem, available at: www.eurachem.org (17 Febraury 2016) 2011.

Beyer, M., Gaj, M., Hamutoko, J., Koeniger, P., Wanke, H., and Himmelsbach, T.: Estimation of groundwater recharge via deuterium labelling in the semi-arid Cuvelai-Etosha Basin, Namibia, Isot. Environ. Health S., 51, 533–552, doi:10.1080/10256016.2015.1076407, 2015.

Braud, I., Bariac, T., Vauclin, M., Boujamlaoui, Z., Gaudet, J. P., Biron, P., and Richard, P.: SiSPAT-Isotope, a coupled heat, water and stable isotope (HDO and $H_2^{18}O$) transport model for bare soil. Part II. Evaluation and sensitivity tests using two laboratory data sets, J. Hydrol., 309, 301–320, doi:10.1016/j.jhydrol.2004.12.012, 2005.

Braud, I., Bariac, T., Biron, P., and Vauclin, M.: Isotopic composition of bare soil evaporated water vapor. Part II: Modeling of RUBIC IV experimental results, J. Hydrol., 369, 17–29, doi:10.1016/j.jhydrol.2009.01.038, 2009.

Caldwell, M. M., Dawson, T. E., and Richards, J. H.: Hydraulic lift: consequences of water efflux from the roots of plants, Oecologia, 113, 151–161, doi:10.1007/s004420050363, 1998.

Christelis, G., Struckmeier, W., Bäumle, R., and Bethune, S.: Groundwater in Namibia: An explanation to the hydrogeological map, 1st ed, Dept. of Water Affairs, Division Geohydrology; Geologigal Survey of Namibia; Namibia Water Corporation; Federal Institute for Geosciences and Mineral Resources, Windhoek, Namibia, Hannover, Germany, 128 pp., ISBN-No.:0-86976-571-X, 2001.

Clark, I. D. and Fritz, P.: Environmental Isotopes in Hydrogeology, Lewis Publishers, Boca Raton, FL, USA, 328 pp., 1997.

Coplen, T., Herczeg, A., and Barnes, C.: Isotope Engineering – Using Stable Isotopes of the Water Molecule to Solve Practical Problems, in: Environmental Tracers in Subsurface Hydrology, Springer, New York, USA, 79–110, doi:10.1007/978-1-4615-4557-6_3, 2000.

Coplen, T. B.: Guidelines and recommended terms for expression of stable-isotope-ratio and gas-ratio measurement results, Rapid Commun. Mass Sp., 25, 2538–2560, doi:10.1002/rcm.5129, 2011.

Craig, H.: Isotopic Variations in Meteoric Waters, Science, 133, 1702–1703, 1961.

Craig, H. and Gordon, L. I.: Deuterium and oxygen 18 variations in the ocean and marine atmosphere. In proc. Stable Isotopes in Oceanographic Studies and Paleotemperatures, 1965, Spoleto, Italy, edited by: E. Tongiogi, 9–130, V. Lishi e F., Pisa, Italy, 1965.

Dawson, T. E.: Hydraulic lift and water use by plants: implications for water balance, performance and plant-plant interactions, Oecologia, 95, 565–574, 1993.

Dawson, T. E.: Determining water use by trees and forests from isotopic, energy balance and transpiration analyses: the roles of tree size and hydraulic lift, Tree Physiol., 16, 263–272, 1996.

Dawson, T. E. and Ehleringer, J. R.: Streamside trees that do not use stream water, Nature, 350, 335–337, 1991.

Dawson, T. E., Mambelli, S., Plamboeck, A. H., Templer, P. H., and Tu, K. P.: Stable Isotopes in Plant Ecology, Annu. Rev. Ecol. Syst., 33, 507–559, doi:10.1146/annurev.ecolsys.33.020602.095451, 2002.

Dincer, T., Al-Mugrin, A., and Zimmermann, U.: Study of the infiltration and recharge through the sand dunes in arid zones with special reference to the stable isotopes and thermonuclear tritium, J. Hydrol., 23, 79–109, doi:10.1016/0022-1694(74)90025-0, 1974.

Dragnich, P. A., Dungca, A. C., Pedleton Noah, L., and Tracy, A. R.: The Cuvelai-Etosha Basin Management Approach; Assessing water resources management in the Iishana sub-basin, Worchester Polytechnic Institute, Desert Research Foundation, Nambia, 2004.

Dubbert, M., Cuntz, M. M., Piayda, A., Maguàs, and Werner, C.: Partitioning evapotranspiration – Testing the Craig and Gordon model with field measurements of oxygen isotope ratios of evaporative fluxes, J. Hydrol., 496, 142–153, doi:10.1016/j.jhydrol.2013.05.033, 2013.

Ehleringer, J. R. and Dawson, T. E.: Water uptake by plants: perspectives from stable isotope composition, Plant Cell Environ., 15, 1073–1082, doi:10.1111/j.1365-3040.1992.tb01657.x, 1992.

Fontes, J., Yousfi, M., and Allison, G. B.: Estimation of long-term, diffuse groundwater discharge in the northern Sahara using stable isotope profiles in soil water, J. Hydrol., 86, 315–327, 1986.

Garvelmann, J., Külls, C., and Weiler, M.: A porewater-based stable isotope approach for the investigation of subsurface hydrological processes, Hydrol. Earth Syst. Sci., 16, 631–640, doi:10.5194/hess-16-631-2012, 2012.

Gazis, C. and Feng, X.: A stable isotope study of soil water: evidence for mixing and preferential flow paths, Geoderma, 119, 97–111, doi:10.1016/S0016-7061(03)00243-X, 2004.

Hendry, M. J., Schmeling, E., Wassenaar, L. I., Barbour, S. L., and Pratt, D.: Determining the stable isotope composition of pore water from saturated and unsaturated zone core: improvements to the direct vapour equilibration laser spectrometry method, Hydrol. Earth Syst. Sci., 19, 4427–4440, doi:10.5194/hess-19-4427-2015, 2015.

Henschel, J. R. and Seely, M. K.: Ecophysiology of atmosspheric moisture in the Namib Desert., Atmos. Res., 87, 362–368, doi:10.1016/j.atmosres.2007.11.015, 2008.

Herczeg, A. L. and Leaney, F. W.: Review: environmental tracers in arid-zone hydrology, Hydrogeol. J., 19, 17–29, 2011.

Kelln, C., Wassenaar L. I., and Hendry, M. J.: Stable Isotopes ($\delta^{18}O$, δ^2H) of Pore Waters in Clay-Rich Aquitards: A Comparison and Evaluation of Measurement Techniques, Ground Water Monit. R., 21, 108–116, 2001.

Kendall, C. and McDonnell, J. J.: Isotopes in catchment hydrology, Elsevier, New York, USA, 2012.

Koeniger, P., Marshall, J. D., Link, T., and Mulch, A.: An inexpensive, fast, and reliable method for vacuum extraction of soil and plant water for stable isotope analyses by mass spectrometry, Rapid Commun. Mass Sp., 25, 3041–3048, doi:10.1002/rcm.5198, 2011.

Koeniger, P., Gaj, M., Beyer, M., and Himmelsbach, T.: Review on soil water isotope based groundwater recharge estimations, Hydrol. Process., doi:10.1002/hyp.10775, accepted, 2016.

Lindenmaier, F. and Christelis, G.: Groundwater for the North of Namibia: Summary Report of Activities of Phase I, Exploration of Ohangwena II Aquifer and Preliminary Isotope Study, Volume 1a, Windhoek, Namibia, 2012.

Lindenmaier, F., Lohe C., and Quinger M.: Groundwater for the North of Namibia: Executive Summary Phase I, Windhoek, Namibia, 2014.

Lee, K. S., Kim, J. M., Lee, D.-R., Kim, Y., and Lee, D.: Analysis of water movement through an unsaturated soil zone in Jeju Island, Korea using stable oxygen and hydrogen isotopes, J. Hydrol., 345, 199–211, doi:10.1016/j.jhydrol.2007.08.006, 2007.

Mendelsohn, J., Jarvis A., Robertson T., Mendelsohn, J., Jarvis, A., and Robertson, T.: A Profile and Atlas of the Cuvelai – Etosha Basin, RAISON; Gondwana Collection, Windhoek, Namibia, 172–170, 2013.

Merlivat, L.: Molecular diffusivities of H216O, HD16O, and H218O in gases, J. Chem. Phys., 69, 2864–2871, doi:10.1063/1.436884, 1978.

Mueller, M. H., Alaoui, A., Kuells, C., Leistert, H., Meusburger, K., Stumpp, C., Weiler, M., and Alewell, C.: Tracking water pathways in steep hillslopes by δ^{18}O depth profiles of soil water, J. Hydrol., 519, 340–352, doi:10.1016/j.jhydrol.2014.07.031, 2014.

Oerter, E., Finstad, K., Schaefer, J., Goldsmith, G. R., Dawson, T., and Amundson, R.: Oxygen isotope fractionation effects in soil water via interaction with cations (Mg, Ca, K, Na) adsorbed to phyllosilicate clay minerals, J. Hydrol., 515, 1–9, 2014

Or, D., Lehmann, P., Shahraeeni, E., and Shokri, N.: Advances in soil evaporation physics – A review, Vadose Zone J., 12, doi:10.2136/vzj2012.0163, 2013.

Orlowski, N., Frede, H.-G., Brüggemann, N., and Breuer, L.: Validation and application of a cryogenic vacuum extraction system for soil and plant water extraction for isotope analysis, J. Sens. Sens. Syst., 2, 179–193, doi:10.5194/jsss-2-179-2013, 2013.

Rambo, J., Lai, C.-T., and Farlin, J.: On-Site Calibration for High Precision Measurements of Water Vapor Isotope Ratios Using Off-Axis Cavity-Enhanced Absorbtion Spectroscopy, J. Atmos. Ocean. Tech., 28, 1448–1457, 2011.

Richard, P. and Shoemaker, C. A.: A Comparison of Chemical and Isotopic Hydrograph Separation, Water Resour. Res., 22, 1444–1454, 1986.

Rothfuss, Y., Vereecken, H., and Brüggemann, N.: Monitoring water stable isotopic composition in soils using gas-permeable tubing and infrared laser absorption spectroscopy, Water Resour. Res., 49, 3747–3755, doi:10.1002/wrcr.20311, 2013.

Rothfuss, Y., Merz, S., Vanderborght, J., Hermes, N., Weuthen, A., Pohlmeier, A., Vereecken, H., and Brüggemann, N.: Long-term and high-frequency non-destructive monitoring of water stable isotope profiles in an evaporating soil column, Hydrol. Earth Syst. Sci., 19, 4067–4080, doi:10.5194/hess-19-4067-2015, 2015.

Savinand, S. M. and Epstein, S.: The oxygen and hydrogen isotope geochemistry of clay minerals, Geochim. Cosmochim. Ac., 34, 25–42, doi:10.1016/0016-7037(70)90149-3, 1970.

Saxena, R. K.: Oxygen-18 fractionation in nature and estimation of groundwater recharge, Uppsala University, Department of Physical Geography, Division of Hydrology, Sweden, 1987.

Scanlon, B. R., Healy, R. W., and Cook, P. G.: Choosing appropriate techniques for quantifying groundwater recharge, Hydrogeol. J., 10, 18–39, doi:10.1007/s10040-001-0176-2, 2002.

Schack-Kirchner, H., Hildebrand, E. E., and von Wilpert, K.: Ein konvektionsfreies Sammelsystem für Bodenluft, Z. Pflanz. Bodenkunde., 156, 307–310, 1993.

Singleton, M. J., Sonnenthal, E. L, Conrad, M. E., DePaolo, D., and Gee, G. W.: Multiphase Reactive Transport Modeling of Seasonal Infiltration Events and Stable Isotope Fractionation in Unsaturated Zone Pore Water and Vapor at the Hanford Site, Vadose Zone J., 3, 775–785, 2004.

Sklash, M. G. and Farvolden, R. N.: The role of groundwater in storm runoff., J. Hydrol., 43, 45–65, 1979.

Skrzypek, G., Mydłowski, A., Dogramaci, S., Hedley, P., Gibson, J. J., and Grierson, P. F.: Estimation of evaporative loss based on the stable isotope composition of water using Hydrocalculator, J. Hydrol., 523, 781–789, 2015.

Soderberg, K., Good, S. P., Wang, L., and Caylor, K.: Stable Isotopes of Water Vapor in the Vadose Zone: A Review of Measurement and Modeling Techniques, Vadose Zone J., 11, 14 pp., doi:10.2136/vzj2011.0165, 2012.

Sutanto, S. J., van den Hurk, B., Dirmeyer, P. A., Seneviratne, S. I., Röckmann, T., Trenberth, K. E., Blyth, E. M., Wenninger, J., and Hoffmann, G.: HESS Opinions "A perspective on isotope versus non-isotope approaches to determine the contribution of transpiration to total evaporation", Hydrol. Earth Syst. Sci., 18, 2815–2827, doi:10.5194/hess-18-2815-2014, 2014.

Sprenger, M., Volkmann, T. H. M., Blume, T., and Weiler, M.: Estimating flow and transport parameters in the unsaturated zone with pore water stable isotopes, Hydrol. Earth Syst. Sci., 19, 2617–2635, doi:10.5194/hess-19-2617-2015, 2015.

Stumpp, C. and Maloszewski, P.: Quantification of preferential flow and flow heterogeneities in an unsaturated soil planted with different crops using the environmental isotope δ^{18}O, J. Hydrol., 394, 407–415, doi:10.1016/j.jhydrol.2010.09.014, 2010.

Sturm, P. and Knohl, A.: Water vapor δ^2H and δ^{18}O measurements using off-axis integrated cavity output spectroscopy, Atmos. Meas. Tech., 3, 67–77, doi:10.5194/amt-3-67-2010, 2010.

Tetzlaff, D., Soulsby, C., Waldron, S., Malcolm, I. A., Bacon, P. J., Dunn, S. M., Lilly, A., and Youngson, A. F.: Conceptualization of runoff processes using a geographical information system and tracers in a nested mesoscale catchment, Hydrol. Process., 21, 1289–1307, doi:10.1002/hyp.6309, 2007.

VanDeVelde, J. H. and Bowen, G. J.: Effects of chemical pretreatments on the hydrogen isotope composition of 2:1 clay minerals, Rapid Commun. Mass. Sp., 27, 1143–1148, doi:10.1002/rcm.6554, 2013.

van Geldern, R. and Barth, J. A.: Optimization of instrument setup and post-run corrections for oxygen and hydrogen stable isotope measurements of water by isotope ratio infrared spectroscopy (IRIS), Limnol. Oceangr.-Meth., 10, 1024–1036, doi:10.4319/lom.2012.10.1024, 2012.

Volkmann, T. H. M. and Weiler, M.: Continual in situ monitoring of pore water stable isotopes in the subsurface, Hydrol. Earth Syst. Sci., 18, 1819–1833, doi:10.5194/hess-18-1819-2014, 2014.

Walker, G. R., Woods, P. H., and Allison, G. B.: Interlaboratory comparison of methods to determine the stable isotope composition of soil water, Chem. Geol., 111, 297–306, doi:10.1016/0009-2541(94)90096-5, 1994.

Wang, L., Caylor, K., and Dragoni, D.: On the calibration of continuous, high-precision δ^{18}O and δ^2H measurements using an off-axis integrated cavity output spectrometer, Rapid Commun. Mass Sp. 23, 530–536, 2009.

Wang, L., Good, S. P., Caylor, K. K., and Cernusak, L. A.: Direct quantification of leaf transpiration isotopic

composition, Agr. Forest Meteorol., 154-155, 127–135, doi:10.1016/j.agrformet.2011.10.018, 2012.

Wassenaar, L. I., Hendry, M. J., Chostner V.L., and Lis G. P.: High Resolution Pore Water ^{2}H and ^{18}O Measurements by $H_2O_{(liquid)}H_2O_{(vapor)}$ Equilibration Laser Spectroscopy, Environ. Sci. Technol., 42, 9262–9267, 2008.

West, A. G., Patrickson, S. J., Ehleringer, J. R.: Water extraction times for plant and soil materials used in stable isotope analysis, Rapid Commun. Mass Sp., 20, 1317–1321, 2006.

Western, A. W., Zhou, S.-L., Grayson, R. B., McMahon, T. A., Blöschl, G., and Wilson, D. J.: Spatial correlation of soil moisture in small catchments and its relationship to dominant spatial hydrological processes, J. Hydrol., 286, 113–134, doi:10.1016/j.jhydrol.2003.09.014, 2004.

Wilson G. W., Fredlund D. G., and Barbour S. L.: The effect of soil suction on evaporative fluxes from soil surfaces., Can. Geotech. J., 34, 145–155, 1997.

Wu, Y., Zhou, H., Zheng, X.-J., Li, Y., and Tang, L.-S.: Seasonal changes in the water use strategies of three co-occurring desert shrubs, Hydrol. Process., 28, 6265–6275, doi:10.1002/hyp.10114, 2014.

Yang Q., Xiao, H., Zhao, L., Zhou, M., and Li, C., Coa, S.: Stable isotope techniques in plant water sources: a review, Science in Cold and Arid Regions, 2, 112–122, 2010.

Zimmermann, U., Münnich K.O., and Roether W.: Downward movement of soil moisture traced by means of hydrogen isotopes, Geoph. Monog. Series, 11, 28–26, 1967.